



**A Bioorthogonal Turn-On Fluorescent Strategy for the
Detection of Lysine Acetyltransferase Activity**

Journal:	<i>ChemComm</i>
Manuscript ID	CC-COM-04-2018-002987
Article Type:	Communication



Journal Name

COMMUNICATION

A Bioorthogonal Turn-On Fluorescent Strategy for the Detection of Lysine Acetyltransferase Activity

Received 00th January 20xx,
Accepted 00th January 20xx

Maomao He,^a Zhen Han,^a Jing Qiao,^a Liza Ngo,^a May P. Xiong,^a Y. George Zheng^{*a}

DOI: 10.1039/x0xx00000x

www.rsc.org/

Lysine acetylation plays vital roles in the regulation of fundamental cellular processes, which is mediated by lysine acetyltransferases (KATs). Developing chemical biology probes for KAT activity detection is of important value in providing improved understanding of their biological functions. We reported a panel of “turn-on” fluorescent probes for sensitive and selective detection of KAT enzymatic activity through a simple mix-and-read format. Combined with bioorthogonal substrate labelling and click chemistry, these probes produced strong “turn-on” fluorescent signals in response to KAT-mediated acylation process. This chemical biology strategy diversifies the assay toolboxes to investigate functions and mechanisms of acetyltransferase enzymes.

Acetylation of lysine residues in proteins represents a pivotal post-translational modification (PTM) conserved from prokaryotes to yeasts and higher organisms. Lysine acetyltransferases (KATs) and lysine deacetylases (KDACs) are two types of enzymes with opposing activities that fine tune the dynamic homeostasis of lysine acetylation.¹ Since their genetic identification in the mid-1990s, KATs have been extensively studied in aspects of structural characterization, biochemical properties, and functions in physiology and pathology. Mounting evidence reveals that dysregulation of KATs is causative to the pathogenesis of many human diseased phenotypes, including neurodegenerative disorders, inflammation, diabetes, and cancer.^{2,3}

Chemical biology probes that detect and quantify KAT activities are essential tools for understanding the scope and depth of acetyltransferase biology.^{4,5} Because of the chemically inert nature of the acetyl group, direct detection of KAT-mediated protein acetylation has been technically challenging, which typically relies on either radioisotope labeling or antibody recognition. The radiometric assays have satisfying sensitivity and reliability.⁶ However, radiometric

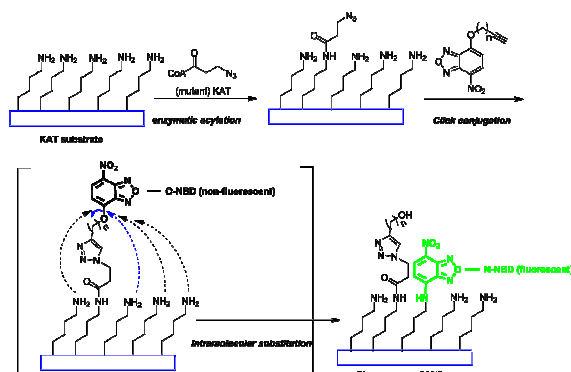
assays suffer from issues such as high cost of radioactive materials, radioactive hazard concerns, and experimental inflexibility (i.e. discontinuous endpoint measurement). Non-radioactive spectroscopic methods such as fluorescent assays, have been explored as alternative strategies.⁷⁻⁹ However, almost all fluorescent methods detect KAT activity by examining the formation of byproduct CoA through either enzyme or chemical reagent coupling. Drawbacks such as background fluorescence, inner filter effect, and incapability for *in vivo* detection limit their biological applications.

We recently explored the bioorthogonal strategy that utilizes synthetic acetyl-CoA analogs and engineered KAT enzymes to provide a chemically maneuverable technology to interrogate substrate profiles of KAT enzymes.¹⁰⁻¹² As an extension of the bioorthogonal labeling strategy, here we created a set of small molecule nitrobenzoxadiazole (NBD) probes to achieve mix-and-read, “turn-on” fluorescence detection of KAT activities. The design takes advantage of the principles that: 1) nucleophilic amino acid residues (lysine, arginine) abundantly exist in histone and non-histone proteins; 2) acetyl-CoA surrogates such as 3-azidopropanoyl CoA (3AZ-CoA) can be excellent bioorthogonal cofactors of specific wild-type or engineered KAT enzymes; and 3) oxygen-linked NBD unit (O-NBD) is non-fluorescent, while nitrogen-linked NBD unit (N-NBD) exhibits strong fluorescence in the wavelength range of 520-550 nm. As a potential fluorophore precursor, the NBD unit has little interference on the ligand-target interaction due to its small size and planar structure. The unique fluorescence-switchable property of NBD makes it a good candidate for probe design,¹³⁻¹⁵ which was recently applied to study KDAC activities.^{14,15} We report here the first application of NBD-based probes to detect KAT activity through integral alignment of bioorthogonal acylation labeling, alkyne-azide click chemistry, and “turn-on” fluorescence. As illustrated in **Scheme 1**, upon KAT-catalyzed bioorthogonal acylation, 3-azidopropanoyl group is transferred from 3AZ-CoA to the substrate, which is further conjugated to an alkyne-O-NBD probe through click chemistry. This event would subsequently trigger a proximity-promoted intramolecular nucleophilic

^a Department of Pharmaceutical and Biomedical Sciences, College of Pharmacy, University of Georgia, Athens, Georgia 30602, United States. E-mail: yzheng@uga.edu

†Electronic Supplementary Information (ESI) available: [details of any supplementary information available should be included here]. See DOI: 10.1039/x0xx00000x

substitution of O-NBD by free amines of adjacent lysine residues in the substrate and thus turns on the fluorescence of the resulting N-NBD motif.



Scheme 1 Illustration of the bioorthogonal “turn-on” fluorescence strategy for KAT activity detection.

As a proof of concept, we chose p300 as the KAT enzyme to design the bioorthogonal “turn-on” fluorescent probes for KAT activity detection. p300 was previously shown to utilize bulky acetyl-CoA surrogates such as 3AZ-CoA to modify histone substrates.^{10–12} Giving that the length of the linker in the NBD probe may affect the efficiency of intramolecular N-substitution reaction, two propargyl NBD probes (**PN-1** and **PN-2**) bearing different lengths of linkers were synthesized from NBD fluoride (**NBD-F**) (Fig. 1a and Schemes S1–S2).¹⁴ Briefly, **NBD-F** was treated with propargyl alcohol or **PTG-1** under basic condition to yield **PN-1** and **PN-2**, respectively. Before testing our designed assay strategy on KAT activity detection, we first studied the fluorescent responses of **PN-1** with the chemical components present in the KAT reaction and the subsequent click reaction. As shown in Fig. S1a–b, The fluorescence intensity of **PN-1** (10 μ M) is similar to **NBD-F** and remained unchanged upon addition of either HEPES buffer (pH 8.0) or 3AZ-CoA, while addition of H4(1-21) substrate peptide (N-terminal 21 residues of histone H4 protein, for full sequence see the SI) brought to a slight increase of the fluorescence intensity. In contrast, when the H4(1-21) peptide was first reacted with 3AZ-CoA in the presence of p300, then treated with **PN-1** together with click reaction cocktail, a dramatic increase of fluorescence signals was observed (Fig. S1b). The results demonstrated that the fluorescence of **PN-1** was selectively turned on only by reacting with the acylated substrate. We then explored the “turn-on” fluorescent responses with respect to the click/N-intramolecular substitution reaction time. In the model study, H4(1-21) was used as the KAT substrate, 3AZ-CoA as the cofactor, and p300 as the KAT enzyme. The KAT enzymatic reaction was allowed to proceed under ambient temperature for 30 min and then the click reaction cocktail in DMSO containing **PN-1** was added. The fluorescence signals were recorded during further incubation at room temperature. As shown in Fig. 1b, the fluorescence signals were weak initially, then increased pronouncedly during incubation and plateaued at 2 h. In

contrast, fluorescence signals of the control group without the treatment of p300 stayed at a very low level. For **PN-2**, the fluorescence increase was slightly higher than that of **PN-1** with the addition of p300, while remained unchanged for the negative control. Likely, the PEG linker in **PN-2** has a higher degree of flexibility and hydrophilicity that helps to reduce the nonspecific intermolecular N-substitution reactions.^{13–15}

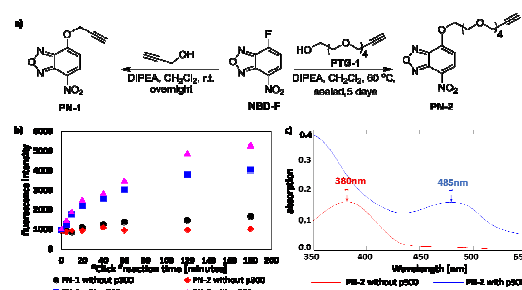


Fig. 1 Synthetic route and click reaction time dependent spectral study of the O-NBD probes. a) Synthesis of **PN-1** and **PN-2**. b) Fluorescence change of **PN-1** (5 μ M) and **PN-2** (5 μ M) with or without adding p300 as a function of click reaction time. H4(1-21) peptide: 5 μ M, 3AZ-CoA: 10 μ M, p300: 0.2 μ M. λ_{ex} = 485 nm. λ_{em} = 545 nm. c) Absorption spectra of **PN-2** with and without adding p300. Enzymatic reaction time was 30 min. click reaction time was 2 h.

Absorption spectral changes of **PN-2** upon KAT acylation reaction were also measured. As seen in Fig. 1c, the spectrum of the reaction mixture containing **PN-2** without the treatment of p300 at enzymatic acylation stage showed a strong absorption peak at 380 nm, which corresponded to the maximum absorption wavelength of the O-NBD group.¹⁵ In contrast, when the enzymatic reaction was performed in the presence of p300, a new absorption peak appeared at 485 nm, which corresponded to the maximum absorption peak of N-NBD group. These experiments together demonstrated that the fluorescence of NBD can be turned on as a function of click reaction time only together with the occurrence of bioorthogonal KAT labeling. We also tested the fluorescence responses of **PN-2** to the acylation of human H3 protein by p300. As expected, the fluorescence spectra showed a steady increase as a function of CuAAC/N-substitution reaction time (Fig. S2).

To further demonstrate that the fluorescence enhancement was caused by O-NBD to N-NBD transformation through reacting with the adjacent amine groups in the substrate, we prepared H4(1-21) peptide with a 3AZ group on its K16 lysine residue [H4(1-21)K16_{3AZ}] and performed click reaction with **PN-2** at pH 2.0 (Fig. S3a). After click reaction (3 h), the pH was adjusted to 8.0 to allow the intramolecular substitution reaction to occur. The process was monitored by HPLC (Fig. S3b). At pH 2.0, no further reaction occurred after the click cycloaddition because amine residues on the substrate peptide were protonated so that intramolecular N-substitution was hindered. After increasing the pH to 8.0, however, amine groups on the substrate were activated which led to the nucleophilic attack on the O-NBD group. Indeed, two new peaks formed on the HPLC chromatogram, which possessed the same mass value (Fig. S3–S4). We also measured the

absorption spectra of the reaction solution at pH 2.0 and 8.0. Our observation showed that the maximum absorption wavelength shifted from 380 nm to 485 nm after pH adjustment (Fig. S3c), which corresponded to the maximum absorption wavelength of the O-NBD and N-NBD group, respectively.¹⁵ By contrast, **PN-2** at two different pH conditions showed identical absorption spectrum (380 nm), which demonstrated that the absorption spectral change was not caused by pH (Fig. S3d). These results together proved our hypothesized click chemistry/N-intramolecular substitution two-step reaction mechanism.

Next, we explored the suitability of **PN-2** as a fluorescent reporter to quantify KAT activity. We first tested the fluorescence response of **PN-2** corresponding to KAT reaction time. For the p300-catalyzed KAT reaction, the enzymatic process was quenched at different time points with the addition of the click reaction cocktail containing **PN-2**. As expected, the fluorescence signals displayed a linear increase with time over the course of 50 min, with a total of 3.2-fold increase (Fig. S5a). The fluorescence signals in response to

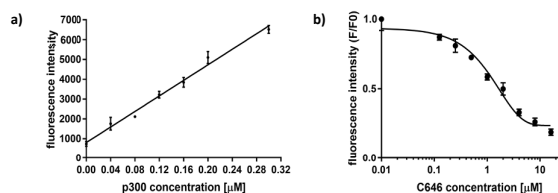


Fig. 2 Turn-on fluorescence of p300 catalyzed acylation. a) p300 concentration dependent fluorescence change of **PN-2**. **PN-2**: 5 μM, H4(1-21): 5 μM, 3AZ-CoA: 5 μM. Enzymatic reaction time was 30 min and “click” reaction time was 3 h. b) Measurement of C646 potency for p300 inhibition.

varying enzyme concentrations were also conducted. As p300 concentrations increased from 0 to 0.32 μM, the fluorescence intensity increased linearly by 6.5-fold (Fig. 2a and Fig. S5b). These results support that this ‘turn-on’ fluorescent assay offers a quantitative approach to detect KAT catalyzed acylation reaction.

We also investigated the capability of **PN-2** to quantify the potency of p300 inhibitors by exposing p300 to a known selective small-molecule KAT inhibitor, C646. Different concentrations of C646 were pre-incubated with p300 for 30 min prior to the addition of H4(1-21) peptide and 3AZ-CoA. The enzymatic reaction was allowed to occur for 1 h, then the click reaction cocktail containing **PN-2** was added to quench the enzymatic reaction and initiate the click reaction at the meantime. The dose-dependent fluorescence signals were measured (Fig. 2b and Fig. S5c) and the data points were fitted to the Hill equation (Equation S1). The IC₅₀ value was calculated to be 1.8 ± 0.1 μM, which was similar to the value reported in the literature.¹⁶ These data clearly proved that the detection platform is effective for quantitative KAT inhibitor evaluations.

With the above encouraging results, we performed fluorescence imaging experiments to examine the labeling efficiency of 3AZ-CoA on the cellular proteome by **PN-1** and **PN-2**. Human embryonic kidney (HEK) 293T cell lysate was incubated with p300 and 3AZ-CoA, followed by CuAAC click

reaction to tag 3AZ-labeled proteins with **PN-2**. As shown in Fig. 3, treatment of the cell lysate with 3AZ-CoA in the presence of p300 and **PN-2** resulted in strong fluorescence signals, indicating efficient labeling of protein substrates with the 3AZ group (lane 1). In contrast, the absence of p300 resulted in very weak fluorescence signals that were close to the negative control without **PN-2** (lane 2 and 4). Similar result was observed when without 3AZ-CoA treatment (lane 3). Additionally, the fluorescence signals became modestly weaker in the presence of inhibitor C646 (5 μM) (lane 5), and stronger when increasing the concentration of p300 (lane 6). The modest effect of C646 may attribute to the high electrophilicity of pyrazolone-furan that lowers its KAT inhibitory activity in cell lysate mixtures.¹⁷ **NBD-F** was also tested as a replacement of **PN-2** and as expected, no fluorescence was observed (lane 7). Combined, these data support that the O-NBD group is essential for the “turn-on” fluorescence, and **PN-2** can be used as a specific reporter to visualize p300 catalyzed histone acylation *in vitro*. Analogously, the fluorescence response of **PN-1** towards HEK 293T cell lysate acylation showed consistent “turn-on” fluorescence results, though the fluorescence signals are slightly lower than that of **PN-2** (Fig. S6). The lower labelling efficiency of **PN-1** than **PN-2** is consistent with the result shown in Fig. 1. Also given that the labeling pattern of **PN-1** in the in-gel fluorescence imaging seems to be a bit different from **PN-2** (Fig. 3 vs Fig. S6), it is quite clear that the flexible and hydrophilic PEG linker in **PN-2** plays a role in fine tuning the N-substitution reaction of the NBD group with proximal amine groups.

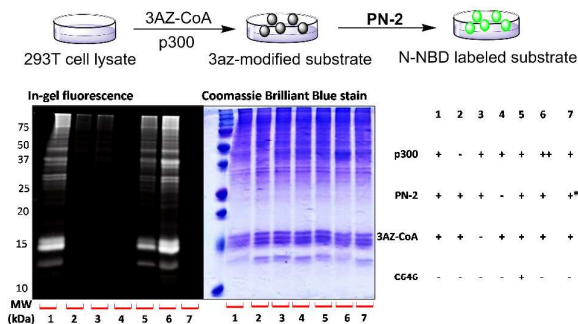


Fig. 3 In-gel fluorescence imaging of protein labelling in 293T cell lysate by **PN-2**. Labelling condition: cell lysate 20 μg, 3AZ-CoA 100 μM, p300 1.2 μM, **PN-2** 150 μM. ++ double the concentration of p300. * **NBD-F** was used instead of **PN-2**.

Although with tremendous success in different areas of chemistry, the cytotoxicity of copper, however, is a potential disadvantage of the CuAAC reaction for biomedical applications.²⁰ Therefore, strain-promoted alkyne-azide cycloaddition (SPAAC) reaction has been used as the alternative for biocompatible labeling. With this idea in mind, a strained O-NBD probe **PN-3** was synthesized in one-step from **BCN-1** with moderate yield (25%) (Fig. 4a). **PN-3** displayed low background fluorescence signals that were similar to **PN-1**, **PN-2** and **NBD-F** (Fig. S1a). In-gel fluorescence visualization was conducted to examine the labeling efficiency of **PN-3** *in vitro*

(Fig. 4b). Clearly, **PN-3** exhibited specific selectivity towards 3AZ-labeled proteins (Fig. 4b, lane 1), this was further corroborated by negative control experiments in which either p300, 3AZ-CoA or **PN-3** was omitted from the reaction mixture (Fig. 4b, lane 2-4), or with the addition of KAT inhibitor C646 (Fig. 4b, lane 5). Additionally, stronger fluorescence signals were observed when the concentration of either **PN-3** or p300 was increased (Fig. 4b, lane 6-7).

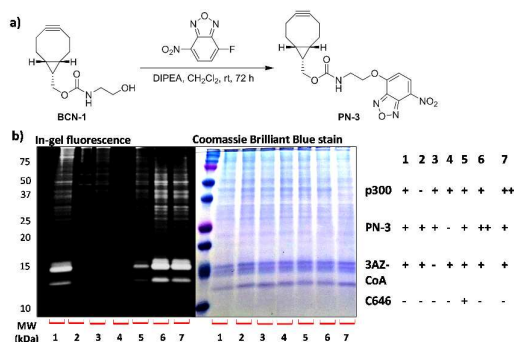


Fig. 4 a) Synthesis of **PN-3**. b) In-gel fluorescence imaging of protein labeling in 293T cell lysate by **PN-3**. Labeling condition: cell lysate 20 μ g, 3AZ-CoA 100 μ M, p300 1.2 μ M, **PN-3** 300 μ M. ++ double the concentration of **PN-3** or p300

Altogether, we designed smart O-NBD probes as “turn-on” fluorescence reporters to achieve sensitive fluorescent detection of p300 enzymatic activity. In combination with bioorthogonal acylation, alkyne-azide click chemistry, and proximity-promoted intramolecular substitution reaction, this technological platform serves as an enabling technology for the detection, quantification, and imaging of KAT activities. While several fluorescent methods have been explored for KAT study,^{7,8,22} the mix-and-read, “turn-on” fluorescence strategy reported herein does not need enzymatic coupling or product separation, and is free of washing procedure, thus greatly reducing assay complexity and expanding throughput capacity. We anticipate this activity-based chemical labeling strategy will find great application in exploring and imaging activities of acetyltransferases.

Conflicts of Interest

There are no conflicts to declare.

Notes and references

1. A. Drazic, L. M. Myklebust, R. Ree and T. Arnesen, *Biochim. Biophys. Acta*, 2016, 1864, 1372-1401.
2. X. J. Yang, *Nucleic Acids Res.*, 2004, 32, 959-976.
3. D. P. Stiehl, D. M. Fath, D. Liang, Y. Jiang and N. Sang, *Cancer Res.*, 2007, 67, 2256-2264.
4. P. A. Cole, *Nat. Chem. Biol.*, 2008, 4, 590-597.
5. M. He, Z. Han, L. Liu and Y. G. Zheng, *Angew. Chem.*, 2017, DOI: 10.1002/anie.201704745.
6. G. W. Aherne, M. G. Rowlands, L. Stimson and P. Workman, *Methods*, 2002, 26, 245-253.

7. Y. Kim, K. G. Tanner and J. M. Denu, *Anal. Biochem.*, 2000, 280, 308-314.
8. T. Kanno, Y. Kanno, R. M. Siegel, M. K. Jang, M. J. Lenardo and K. Ozato, *Mol. Cell*, 2004, 13, 33-43.
9. A. W. Sorum, J. H. Shrimp, A. M. Roberts, D. C. Montgomery, N. K. Tiwari, M. Lal-Nag, A. Simeonov, A. Jadhav and J. L. Meier, *ACS Chem. Biol.*, 2016, 11, 734-741.
10. Y.-Y. Yang, J. M. Ascano and H. C. Hang, *J. Am. Chem. Soc.*, 2010, 132, 3640-3641.
11. C. Yang, J. Mi, Y. Feng, L. Ngo, T. Gao, L. Yan and Y. G. Zheng, *J. Am. Chem. Soc.*, 2013, 135, 7791-7794.
12. Z. Han, C. W. Chou, X. Yang, M. G. Bartlett and Y. G. Zheng, *ACS Chem. Biol.*, 2017, 12, 1547-1555.
13. T. Yamaguchi, M. Asanuma, S. Nakanishi, Y. Saito, M. Okazaki, K. Dodo and M. Sodeoka, *Chemical Science*, 2014, 5, 1021-1029.
14. I. N. Gober and M. L. Waters, *J. Am. Chem. Soc.*, 2016, 138, 9452-9459.
15. Y. Xie, J. Ge, H. Lei, B. Peng, H. Zhang, D. Wang, S. Pan, G. Chen, L. Chen, Y. Wang, Q. Hao, S. Q. Yao and H. Sun, *J. Am. Chem. Soc.*, 2016, 138, 15596-15604.
16. Y. T. Han, H. Li, Y. F. Hu, P. Li, H. X. Wang, Z. Nie and S. Z. Yao, *Anal. Chem.*, 2015, 87, 9179-9185.
17. J. H. Shrimp, A. W. Sorum, J. M. Garlick, L. Guasch, M. C. Nicklaus and J. L. Meier, *ACS Med. Chem. Lett.*, 2016, 7, 151-155.
18. L. M. Lasko, C. G. Jakob, R. P. Edalji, W. Qiu, D. Montgomery, E. L. Digiammarino, T. M. Hansen, R. M. Risi, R. Frey, V. Manaves, B. Shaw, M. Algire, P. Hessler, L. T. Lam, T. Uziel, E. Faivre, D. Ferguson, F. G. Buchanan, R. L. Martin, M. Torrent, G. G. Chiang, K. Karukurichi, J. W. Langston, B. T. Weinert, C. Choudhary, P. de Vries, J. H. Van Drie, D. McElligott, E. Kesicki, R. Marmorstein, C. H. Sun, P. A. Cole, S. H. Rosenberg, M. R. Michaelides, A. Lai and K. D. Bromberg, *Nature*, 2017, 550, 128-+.
19. V. M. Richon, S. Emiliani, E. Verdin, Y. Webb, R. Breslow, R. A. Rifkin and P. A. Marks, *Proc. Natl. Acad. Sci. U. S. A.*, 1998, 95, 3003-3007.
20. K. Merker, D. Hapke, K. Reckzeh, H. Schmidt, H. Lochs and T. Grune, *BioFactors*, 2005, 24, 255-261.
21. C. Choudhary, B. T. Weinert, Y. Nishida, E. Verdin and M. Mann, *Nat. Rev. Mol. Cell Biol.*, 2014, 15, 536-550.
22. P. R. Thompson, D. Wang, L. Wang, M. Fulco, N. Pediconi, D. Zhang, W. An, Q. Ge, R. G. Roeder, J. Wong, M. Levrero, V. Sartorelli, R. J. Cotter and P. A. Cole, *Nat. Struct. Mol. Biol.*, 2004, 11, 308-315.